JOURNAL OF AIRCRAFT
Vol. 42, No. 1, January–February 2005

Separated Shock–Boundary-Layer Interaction Control Using Streamwise Slots

H. A. Holden* and H. Babinsky†
Cambridge University, Cambridge, England, U.K.

Experiments have been performed to assess the potential of discretely placed arrays of streamwise slots to control a separated normal shock wave–turbulent boundary-layer interaction. The supersonic blowdown wind tunnel was operated at a Mach number of 1.5 and a freestream Reynolds number of 26×10^6 m^{-1}. At $M = 1.5$ slot control bifurcated the shock to give a λ shock structure that was significantly larger than that seen without control. The effect on the shock was fairly two-dimensional and persisted in the region between control devices, showing that three-dimensional control devices can have a global effect on the shock structure. In addition, slot control altered the nature of the separated boundary layer from a two-dimensional separation bubble to give highly three-dimensional regions of attached and separated flow. There is evidence that slot control also introduced streamwise vortices, which may help delay or prevent downstream separation.

Nomenclature

M = Mach number
P = pressure
R = reattachment
S = separation
X = streamwise coordinate, mm
Y = vertical coordinate, mm
Z = spanwise coordinate, mm
β = shock angle
δ = boundary-layer thickness
λ = lambda shock structure

Subscripts

s = shock
0 = total conditions
1 = upstream of shock
2 = downstream of main shock
∞ = freestream

Introduction

NORMAL shock wave–boundary-layer interactions (SBLIs) occur in a wide variety of high-speed flow applications, for example, jet engine air intakes with mixed supersonic compression (Fig. 1). Here the flow is decelerated through a series of oblique shocks and a terminating normal shock. Each interaction between a shock wave and the boundary layer increases total pressure losses, reducing engine efficiency. The interactions also cause inlet distortion and in extreme cases can lead to engine unstart. In practice these detrimental effects are avoided using boundary-layer bleed. However, this causes bleed drag penalties and may even strengthen the shock, thus increasing stagnation pressure losses. Methods of controlling and weakening the SBLI and its detrimental effects would be beneficial for engine performance.

A variety of SBLI control methods have been studied in connection with flows over transonic wings. The control methods tend to fall into two main categories. The first concentrates on weakening the shock by splitting it to give a bifurcated λ shock structure, which reduces the total pressure losses behind the shock system. Examples of this method include passive devices[1–5] and two-dimensional surface bumps.[6,7] The second method aims to energize the boundary layer, making it less susceptible to the detrimental effect of the shock wave. Examples of this method include blowing[5] and suction[8,9] and the use of vortex generators.[10,11] A recent investigation found that arrays of streamwise slots can have beneficial effects when placed underneath an SBLI.[12] A detailed study of slot control at $M_s = 1.3$ found that these act in a similar manner to passive control, causing a bifurcated λ shock structure. This bifurcation persisted in the region between control devices.[13] Such a finding is advantageous because it shows that discrete three-dimensional devices can give global shock control. Moreover, the viscous losses were limited to narrow regions behind the devices and there was also evidence of vortical flow in these areas. The main features of the flow structure are summarized in Fig. 2.[14] More recently, other arrays of three-dimensional control devices such as grooves and sub-boundary-layer three-dimensional bumps have been investigated. These were found to have effects on the shock similar to slot control, with viscous losses again confined to narrow regions behind the devices.[15,16]

SBLIs in engine intakes tend to occur at higher Mach numbers than those seen on transonic aerofoils. In addition, the SBLI is separated, a change in flow physics that might affect the behavior and physical mechanism of the control devices. It was therefore decided to investigate shock control using three-dimensional devices at the higher Mach number of $M_s = 1.5$. Because the slot control case is the best understood of the three-dimensional devices investigated at $M_s = 1.3$ so far, it was decided to concentrate on this device at the higher Mach number. Some information from basic experiments using a two-dimensional bump is also shown to illustrate flow behavior.

Experimental Arrangement

The experimental investigation was performed in a blowdown supersonic wind tunnel at the University of Cambridge. The upstream throat consists of a shaped liner, which gives uniform parallel flow with a nominal Mach number of 1.5 ahead of the shock. There was an adjustable aerofoil in the second throat. The stagnation pressure and temperature are 1.8×10^5 Pa and 295 K, respectively. The tunnel arrangement and control region are shown in Fig. 3a. The working section is 114 mm wide, 172 mm long, and 178 mm tall. Manual adjustment of the freestream stagnation pressure and the second throat allows a recovery shock to be held at a given location in the parallel section of the working section, giving run times of approximately 45 s. Three shock positions were investigated, approximately one-third, one-half, and two-thirds of the way along the control devices. This paper concentrates on the middle shock location, $X = 0$ mm

Received 20 August 2003; revision received 19 December 2003; accepted for publication 23 December 2003. Copyright © 2004 by H. A. Holden and H. Babinsky. Published by the American Institute of Aeronautics and Astronautics, Inc., with permission. Copies of this paper may be made for personal or internal use, on condition that the copier pay the $10.00 per-copy fee to the Copyright Clearance Center, Inc., 222 Rosewood Drive, Danvers, MA 01923; include the code 0021-8669/05 $10.00 in correspondence with the CCC.

*Member, Department of Engineering. Student Member AIAA.
†Member, Department of Engineering. Member AIAA.

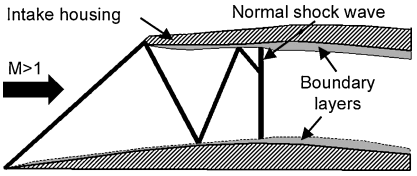

Fig. 1 SBLI in a supersonic engine intake.

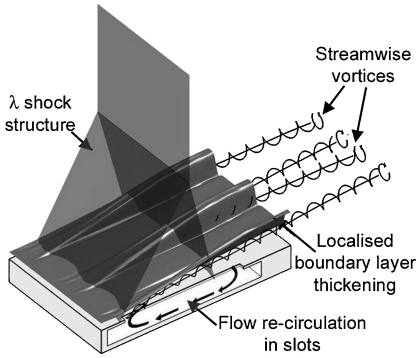

Fig. 2 Structure of a shock–boundary-layer interaction controlled by streamwise slots, $M_s = 1.3$.[14]

(see Fig. 3b for the coordinate system used). The experiments made use of the interaction between the shock wave and the naturally grown turbulent boundary layer on the tunnel floor. The incoming boundary-layer thickness is about 6 mm and the Reynolds number based on boundary-layer displacement thickness is 26,000.

Two types of control device were investigated, an array of streamwise slots and a sub-boundary-layer two-dimensional bump (see Figs. 3c and 3d). Both types of device were 100 mm long and started at the same streamwise position, $X = -50$ mm. The slot control device consisted of an array of three 4-mm-wide slots over a 38-mm-deep cavity. The middle slot was centered on $Z = 0$ mm and the spacing between slot centerlines was 44 mm. The two-dimensional bump had a 5-deg deflection angle and spanned the tunnel, except for a 5-mm gap at either side to allow for the sidewall boundary layers. The maximum height of the two-dimensional bump is 5.25 mm, compared to an upstream uncontrolled boundary-layer thickness of 6 mm. The plateau on the top of the bump started at $X = 10$ mm and was 15 mm long.

Surface pressure measurements were made using Druck PDCR-200 miniature pressure transducers connected to pressure tappings. Figure 3b shows the location of these. The shock is located in the center of the working section at $X = 0$ mm. Boundary-layer traverses were performed upstream and downstream of the interaction using a flat-headed pitot probe (dimensions 1.61×0.131 mm) connected to a pressure transducer. Total pressure traverses were made downstream of the interaction at $X = 90$ mm using a round-headed pitot probe (external diameter 1.1 mm, internal diameter 0.5 mm). Surface oilflow visualization was performed using a paraffin, titanium dioxide, and oleic acid mixture.

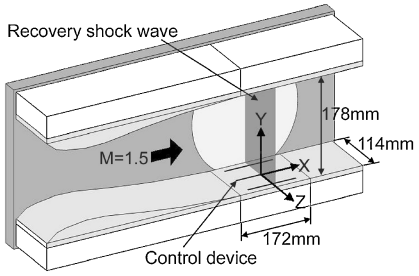

a) Wind-tunnel arrangement

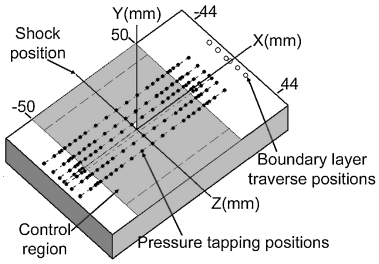

b) Coordinate system

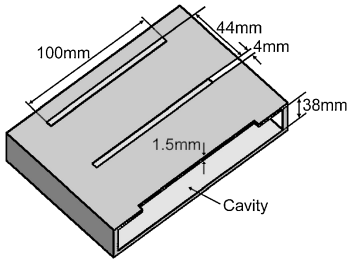

c) Cross section of slot

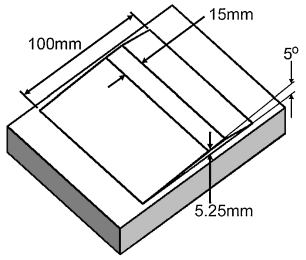

d) Two-dimensional bump

Fig. 3 Experimental arrangement.

Experimental Accuracy

The experimental error in the surface static and pitot pressures measured using the transducers is of the order of $\pm 1\%$. The traverse gear used to measure boundary-layer profiles had an accuracy better than 0.1 mm (0.5% of the boundary-layer thickness). A degree of unsteadiness was observed in the shock wave, resulting in an error in streamwise location of the order of 3 mm, which is typically 3% of the control device.

Results

Uncontrolled Interaction, $M_s = 1.5$

At $M_s = 1.5$ the schlieren picture (Fig. 4) indicates that the flow has separated; there is a small λ structure where the shock foot interacts with the boundary layer. Slight imperfections in the tunnel wall cause a spurious wave to emanate from upstream of the interaction. There is also a number of weak waves emanating from pressure tapping points on the surface. Neither has a significant effect on the flow before the SBLI, as can be seen from the nearly constant value of the wall pressure measurements before the shock (Fig. 5). The wall pressure measurements for the uncontrolled case do not exhibit a plateau at the location of the λ shock, because the length of the separated region is still quite short. The surface oilflow visualization shows a distinct separation line (unfortunately slightly smeared during tunnel shutdown) and a region where reattachment probably occurs (Fig. 6a). The location of the separation line agrees well with the start of the λ structure seen in the schlieren picture; the reattachment region occurs slightly after the rear leg. The separation line is approximately normal to the freestream direction and fairly two-dimensional in the center of the tunnel, but there is curvature at the edges due to the interaction with the sidewall boundary layers. The separations at the tunnel sidewalls occupy approximately 8% of the tunnel span at the shock position.

The flow structure is in agreement with the separated SBLI structure defined by Seddon,[17] with a slip line separating the higher velocity flow that has passed through the bifurcated interaction from the lower velocity flow that has passed through the main shock.

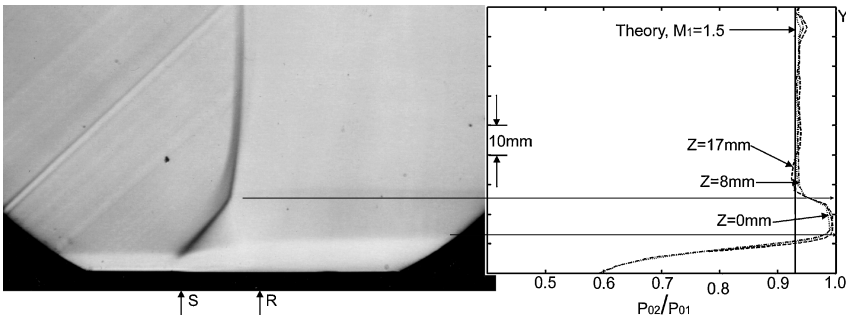

Fig. 4 Schlieren picture and total pressure traverses at $X = 90$ mm, uncontrolled SBLI.

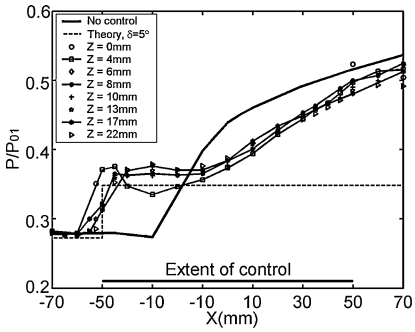

a) Streamwise slots

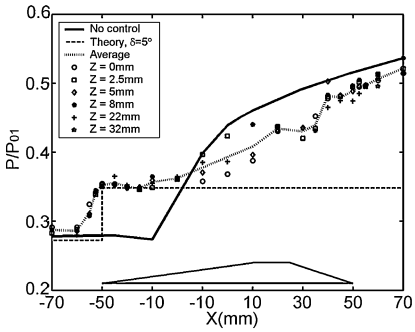

b) Two-dimensional bump

Fig. 5 Wall pressure measurements.

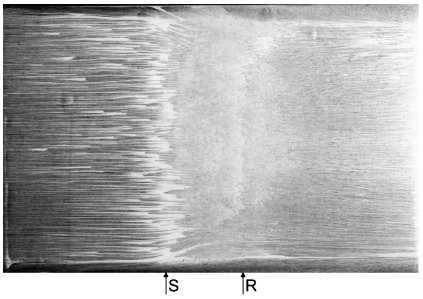

a) No control

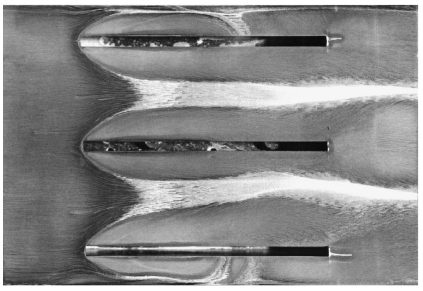

b) Slot control

Fig. 6 Surface oilflow visualization; both images show the full spanwise width of the working section.

As expected the flow downstream of the λ shock structure has reduced total pressure losses compared to the flow behind the normal shock (Fig. 4). The triple point is about 28 mm above the tunnel floor, as measured from the schlieren picture, and between 26 and 28 mm as measured from the total pressure traverses. It can be seen from the similarity of the total pressure traverses at $Z = 0$, 8, and 17 mm that the shock structure and the boundary layer are fairly two-dimensional. The boundary layer upstream of the shock is about 6 mm thick and the velocity profile is fairly full (Fig. 7a). After the shock the boundary layer has almost doubled in thickness to about 13 mm and is much less full (Fig. 7a). With increasing streamwise position from the shock the velocity profile gradually becomes fuller, though at $X = 90$ mm it has still not recovered fully. Velocity profiles taken across the span of the tunnel at $X = 90$ mm show that there is slight spanwise variation in the flow, although the similarity of the profiles at $Z = \pm 22$ mm suggests that the boundary layer is fairly symmetrical about the tunnel centerline (Fig. 7b). The three-dimensionality could be due to the large separations at the tunnel sidewalls seen in the surface oilflow visualization (Fig. 6a). However, in general the variation in the boundary-layer profiles is slight, and the boundary layer appears to be quasi-two-dimensional.

Slot Control, $M_s = 1.5$

Shock Structure

As can be seen from the schlieren picture, the slot control devices split the shock to give a bifurcated λ shock structure that is significantly larger than that observed without control (Fig. 8). The wall pressure measurements reflect this result; there is an initial pressure rise associated with the leading shock, a distinct plateau, and then a second pressure rise associated with the rear shock leg (Fig. 5a). The slots work by a method termed passive shock control[5] whereby flow recirculates from the high-pressure region downstream of the shock to the low-pressure region ahead of it and generates a viscous bubble. The bubble deflects the outer flow in a manner similar to a two-dimensional surface bump. Comparing the schlieren images and wall pressure measurements for slot control with those for a two-dimensional bump clearly demonstrates this (Figs. 5, 8, and 9). "Passive" control methods are so called because they are self-actuated and do not require a pump or moving device to make them work. In the case of passive shock control the process is "driven" by the pressure difference across the shock. For this reason passive shock control only works when the shock is located over the porous cavity; when the shock is elsewhere the control effect is "switched off" and the shock is no longer bifurcated.

There are significant differences in the nature of the shock structure produced by the slots and the two-dimensional bump. The leading leg of the shock generated by the two-dimensional bump is sharp, with little blurring in the schlieren picture, indicating that the shock is fairly two-dimensional across the tunnel span. The wall pressure measurements confirm this result, showing little variation in the leading shock with spanwise position (Fig. 5b). This result is to be expected given that the bump is a two-dimensional device. By contrast, the shock leading leg is blurred in the schlieren picture of the slot control case (Fig. 8). The blurring is explained

by examining the wall pressure measurements, where it can be seen that the initial pressure rise moves slightly downstream with increasing spanwise distance from the slot (Fig. 5a). This result indicates that the shock structure is relaxing back toward the uncontrolled case in the region between control devices. However, the surface pressure map shows that this change is very gradual and that the shock structure generated by the slots is mainly two-dimensional (Fig. 10).

Boundary-Layer Behaviour over Devices

The disparity in the performance of the two control devices can, to a large extent, be explained by the different effects they have on the boundary layer. The boundary layer "rises up" over the two-dimensional bump so the outer flow sees the boundary-layer edge as a corner, which it negotiates by turning through an oblique shock. The shock angle β for the two-dimensional bump is 48 deg, implying a flow deflection of 5 deg. This is confirmed by the wall pressure measurements, which rise to the theoretical value for an oblique shock generated by a 5-deg deflection angle (Fig. 5b). This result is not unexpected, given that the ramp angle for the two-dimensional bump is 5 deg, but does indicate that there is little boundary-layer attenuation. In the slot control case β varied from 47 to 50 deg, which suggests that the flow deflection angle experienced by the outer flow lies between about 4.3 and 6.4 deg. This is further evidence that the slots create a degree of three-dimensionality in the shock structure (and in the boundary layer). It also shows that the "passive" effect is capable of generating large flow deflection effects. Another interesting feature of the shock structure generated by the slots is the slight reexpansion after the initial shock seen in the wall pressure measurements closest to the slot at $Z = 4$ mm. Based on other studies of passive control using arrays of grooves,[14,15,18] which have shown similar, though much stronger, reexpansions, it can be conjectured that this reexpansion is due to a localized region where the blowing is initially strong before reducing in severity in the downstream direction. The effect of this is to cause the boundary layer to thicken and then relax, creating a concave boundary-layer edge, which generates a reexpansion. However, this appears to be a very limited effect, as the reexpansion is not seen at greater spanwise distances from the slot. This result does suggest that in the very localized region over the slot, where wall pressure measurements were not possible, more pronounced regions of three-dimensionality may exist with higher peak pressures and a stronger reexpansion.

Shock "Pinning"

Both control cases generate weak secondary shocks after the main λ structure, indicating that the downstream flow is only just subsonic and easily reaccelerated to supersonic values by boundary-layer growth. A further interesting feature of both control devices is that once the main shock is in the control region, the leading leg

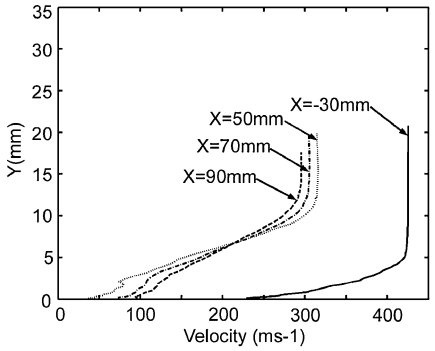

a) Streamwise, Z = 0 mm

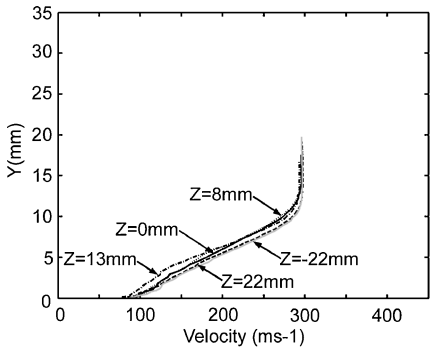

b) Spanwise, X = 90 mm

Fig. 7 Boundary-layer velocity profiles, uncontrolled SBLI.

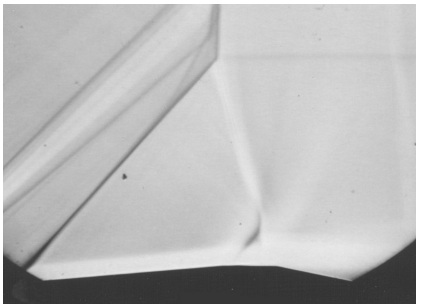

Fig. 9 Schlieren picture, two-dimensional bump.

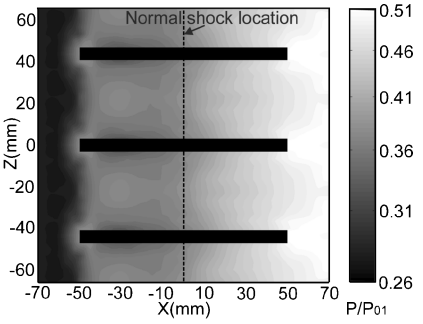

Fig. 10 Surface pressure map, slot controlled SBLI.

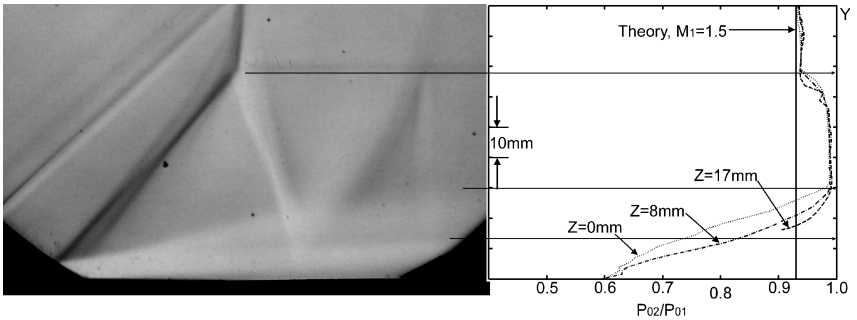

Fig. 8 Schlieren picture and total pressure traverses at X = 90 mm, slot controlled SBLI.

of the λ structure is fixed to the start of the control device no matter the position of the main shock. In the case of slot control this means that provided the main shock is not too close to the tail of the slot (which would prevent downstream flow from recirculating into the cavity) the control device is always switched on, with the size of the λ structure increasing as the shock moves downstream. This shock pinning could be useful for controlling unsteady shocks. While the shock leading leg is also pinned to the start of the two-dimensional bump it can be seen that there are reexpansions over the corners at $X = 10$ and 25 mm, near the rear shock leg. There also appears to be boundary-layer separation downstream of the second of these corners. These flow features are obviously undesirable and would be detrimental to the two-dimensional bump's performance and show that in its present form the two-dimensional bump is only effective when the rear leg of the shock is on the ramp section of the device (before $X = 10$ mm). Note that the separation also made it difficult to hold the shock steady over the two-dimensional bump, which affected the wall pressure measurements over the rear half of the device. (For this reason an average wall pressure measurement is plotted in Fig. 5b). The shock unsteadiness did not significantly affect the wall pressure measurements over the front half of the device due to the shock pinning previously mentioned. If the two-dimensional bump were to be developed further it would be designed to avoid separation and the reexpansions. However, in its present form the two-dimensional bump has been useful to illustrate the flow physics of shock control.

Downstream Development of the Boundary Layer

A further indication of the three-dimensionality caused by the slot control case is the effect on the boundary layer downstream of the interaction. It can be seen, from examining the schlieren picture and total pressure traverses, that there are localized regions of boundary-layer thickening close to the slot (Fig. 8). This is more obvious in the boundary-layer velocity profiles (Fig. 11a). Close to the control device the boundary layer is thicker and much less full. As the flow develops downstream of the interaction the boundary layer farther from the control devices becomes thicker (see Fig. 8). In contrast, closer to the control device the boundary layer thickens only slightly and the velocity profile becomes fuller (Fig. 11b).

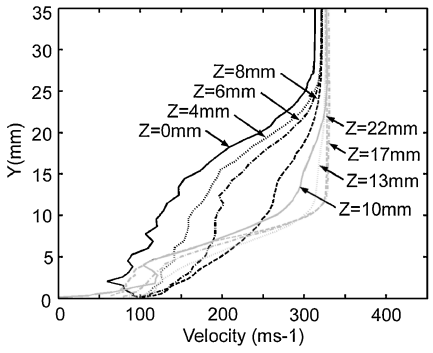

a) Spanwise, $X = 50$ mm

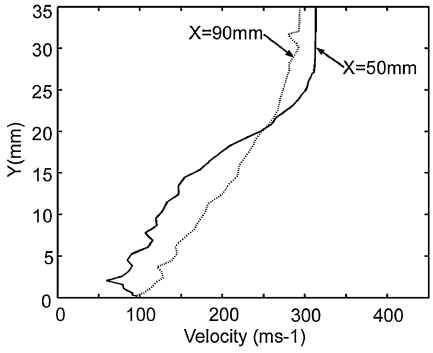

b) Streamwise, $Z = 0$ mm

Fig. 11 Boundary-layer velocity profiles, slot controlled SBLI.

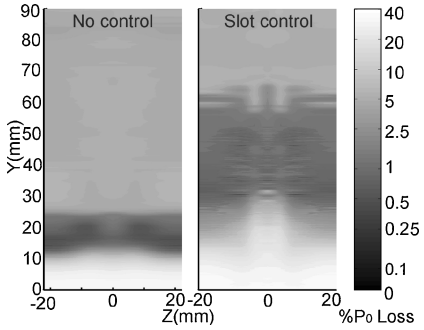

Fig. 12 Total pressure maps, $X = 90$ mm.

These results suggest that there is flow moving in the spanwise direction. Further evidence of sideways motion is seen in the surface oilflow visualization (Fig. 6b) where there is distinct flow turning downstream of the slots. This closely resembles the surface oilflow visualization observed for slot control at Mach 1.3; at this Mach number crossflow velocity profiles were obtained from three hole probe traverses.[15] It was found that flow moved away from the slot in the inner regions of the boundary layer and toward the slot in the outer regions of the boundary layer. There were no spanwise velocity components at $Z = 0$ or 22 mm, indicating that these are planes of symmetry. A computational study of groove control (which closely resembles slot control) at Mach 1.3 produced simulated surface oilflow visualization that closely resembled experimental results and showed that the flow turning was due to the presence of streamwise vortices.[18] Comparing the results from these earlier investigations at Mach 1.3, it could be deduced that at Mach 1.5 the slots behave in a similar manner and are introducing streamwise vortices downstream of the interaction. Such a feature could be desirable in delaying or preventing separation farther downstream. The surface oilflow visualization also shows distinct three-dimensional separations around the slots. In between the control regions flow retardation is evident (indicated by the thick white oilflow deposits in this region) but there is no separation. The control has effectively changed the shape of the separation region from an almost uniform spanwise bubble into highly three-dimensional regions of attached and separated flow.

Total Pressure Losses

The total pressure maps (taken downstream of the interaction at $X = 90$ mm) show that the streamwise slots increase the region of reduced total pressure losses compared to the uncontrolled case; however, the slots also increase the viscous losses by thickening the boundary layer (Fig. 12). This thickening is confined to fairly narrow regions behind the devices, but these regions do spread in the spanwise direction with increasing streamwise distance from the slots. However, the surface pressure plots show that the shock only relaxes gradually between the devices. Optimization of the slots should therefore concentrate on increasing their spanwise spacing to reduce the viscous losses while retaining the reduction in total pressure losses. In addition the slots could be made longer so that the λ shock structure can be made larger. Unfortunately it is not possible to increase the slot spacing at the University of Cambridge due to tunnel-width constraints. Holding the shock farther downstream over the slots would improve the reduction in total pressure losses further. (The bifurcated λ shock structure would be larger, because the shock leading leg is pinned to the start of the device.) An alternative method of reducing the viscous losses might be to use bleed downstream of the slots. This could be done in confined regions directly behind the slots, reducing the bleed drag penalties, and might have the added advantage of further strengthening the streamwise vortices.

Conclusions

Three-dimensional control devices have been shown to give a bifurcated λ shock structure, which extends beyond the control device. This indicates that, correctly spaced, arrays of three-dimensional

devices could have a global control effect and lead to reduced stagnation pressure loss. Slot control is currently the most effective and best understood control method. Comparison with slot control at $M = 1.3$ suggests that moving to a higher shock Mach number with separated flow does not appear to alter the fundamental mechanics of the slot control device.[13–15] However, slot control appears to have totally altered the flow structure, changing a two-dimensional separation bubble into highly three-dimensional regions of attached and separated flow. The slots also introduce streamwise vortices downstream of the SBLI, which might be beneficial for delaying or preventing downstream separation. In addition it is found that the leading leg of the λ shock structure is pinned to the start of the control device, which might be of benefit for controlling unsteady shocks. The devices require further optimization to improve their performance, including increasing the spanwise spacing and holding the shock farther downstream over the device.

Acknowledgments

Both authors thank the Engineering and Physical Sciences Research Council (EPSRC) UK, GKN Westland, Thales Underwater Systems and Dr. Clyde Warsop at BAE SYSTEMS for their continuing interest and support. The authors are indebted to Joyce Moore, a 4th year student at the University of Cambridge Department of Engineering, for her project work on the $M = 1.5$ slot control case.

References

[1]Chokani, N., and Squire, L. C., "Transonic Shockwave/Turbulent Boundary Layer Interactions on a Porous Surface," *Aeronautical Journal*, Vol. 97, May 1993, pp. 163–170.

[2]Gibson, T., Babinsky, H., and Squire, L., "Passive Control of Shock Wave–Boundary-Layer Interactions," *Aeronautical Journal*, Vol. 104, No. 1033, 2000, pp. 129–140.

[3]Raghunathan, S., "Passive Control of Shock Boundary Layer Interaction," *Progress in Aerospace Sciences*, Vol. 25, No. 3, 1988, pp. 271–296.

[4]Thiede, P., and Krogmann, P., "Passive Control of Transonic Shock/Boundary Layer Interactions," *Proceedings of the Fluid Mechanics and Its Applications, IUTAM Symposium Transonicum III*, IUTAM, edited by J. Zierep and H. Oertel, Springer-Verlag, Berlin, Germany, 1988, pp. 379–388.

[5]Delery, J., Shock Wave/Turbulent Boundary Layer Interaction and Its Control, *Progress in Aerospace Sciences*, Vol. 22, No. 4, 1985, pp. 209–280.

[6]Stanewsky, E., "Aerodynamic Benefits of Adaptive Wing Technology," *Aerospace Science and Technology*, Vol. 4, No. 7, 2000, pp. 439–452.

[7]Delery, J., "Shock Phenomena in High Speed Aerodynamics: Still a Source of Major Concern," *Aeronautical Journal*, Vol. 103, No. 1019, 1999, pp. 19–34.

[8]Babinsky, H., "Active Control of Swept Shock Wave/Boundary Layer Interactions," Interactions Drag Reduction by Shock and Boundary Layer Control: Results of the Project Euroshock II, edited by E. Stanewsky, Springer-Verlag, Berlin, pp. 179–204.

[9]Krogmann, P., Stanewsky, E., and Thiede, P., "Effects of Suction on Shock/Boundary-Layer Interaction and Shock-Induced Separation," *Journal of Aircraft*, Vol. 22, No. 1, 1985, pp. 37–42.

[10]Inger, G., and Siebersma, T., "Computational Simulation of Vortex Generator Effects on Transonic Shock/Boundary-Layer Interaction," *Journal of Aircraft*, Vol. 26, No. 8, 1989, pp. 697–698.

[11]Wortman, A., "Reduction of Fuselage Form Drag by Vortex Flows," *Journal of Aircraft*, Vol. 36, No. 3, 1999, pp. 501–506.

[12]Smith, A., and Babinsky, H., Fulker, J., and Ashill, P., "Experimental Investigation of Transonic Aerofoil Shock/Boundary Layer Interaction Control Using Streamwise Slots," *Proceedings of the Fluid Mechanics and Its Applications, IUTAM Symposium Transsonicum IV*, edited by H. Sobieczky, Kluwer, Dordrecht, The Netherlands, 2002, pp. 285–290.

[13]Smith, A., Babinsky, H., Fulker, J., and Ashill, P., "Control of Normal Shock Wave/Turbulent Boundary-Layer Interaction Using Streamwise Slots," AIAA Paper 01-0739, Jan. 2001.

[14]Smith, A. N., Holden, H. A., Babinsky, H., Ashill, P., and Fulker, J., "Control of Normal Shock Wave/Turbulent Boundary Layer Interactions Using Streamwise Grooves," AIAA Paper 02-0978, Jan. 2002.

[15]Smith, A., Babinsky, H., Fulker, J., and Ashill, P., "Normal Shock Wave-Turbulent Boundary-Layer Interactions in the Presence of Streamwise Slots and Grooves," *Aeronautical Journal*, Vol. 106, No. 1063, 2002, pp. 493–500.

[16]Holden, H., and Babinsky, H., "Shock/Boundary Layer Interaction Control Using 3D Devices," AIAA Paper 03-0447, Jan. 2003.

[17]Seddon, J., "The Flow Produced by Interaction of a Turbulent Boundary Layer with a Normal Shock Wave of Strength Sufficient to Cause Separation," R&M 3502, Aeronautical Research Council, London, March 1960.

[18]Smith, A., Babinsky, H., and Dhanasekaran, C., Savill, M., and Dawes, B., "Computational Investigation of Groove Controlled Shock Wave/Boundary Layer Interaction," AIAA Paper 03-0446, Jan. 2003.